iJRASET
International Journal For Research in Applied Science and Engineering Technology



INTERNATIONAL JOURNAL FOR RESEARCH

IN APPLIED SCIENCE & ENGINEERING TECHNOLOGY

Volume: 14 **Issue:** XI **Month of publication:** November 2026

DOI: https://doi.org/10.22214/ijraset.2026.85666

www.ijraset.com

Call: 08813907089 | E-mail ID: ijraset@gmail.com

International Journal for Research in Applied Science & Engineering Technology (IJRASET)
ISSN: 2321-9653; IC Value: 45.98; SJ Impact Factor: 7.538
Volume 14 Issue XI Nov 2026- Available at www.ijraset.com

Aerodynamic Optimization of Building using ETABS

Ravikumar Marali[1], Namrata S Naragundkar[2]
[1, 2]*GM School of Advanced Studies, GM University, Davanagere - 577 006, Karnataka, India*

Abstract: ***This study explores the aerodynamic optimization of building forms using ETABS software. Five distinct geometric configurations were analyzed to assess their impact on wind-induced effects: a sharp corner square form, a recessed corner form, a chamfered corner form, a rounded corner form, and an optimized octagonal form. By modeling and evaluating these forms, the research aims to identify design modifications that can effectively reduce wind loads and improve structural performance. The comparative analysis provides insights into how architectural geometry influences aerodynamic behavior, informing future high-rise building designs for enhanced wind resistance and structural efficiency.***
Keywords: Aerodynamics, ETABS, Optimization, Storey Drift, Storey Forces.

I. INTRODUCTION

As a building gets taller, lateral loading becomes more dominant, as wind acts over a larger surface area and higher loads are concentrated towards the bottom. Simultaneously, the mass and stiffness of the structure can be reduced with the use of high-strength concrete and efficient framing systems, making the response to wind more prominent. This makes the design of tall buildings more complex, as it requires the integration of the architectural form, the dynamics of the structure, the conditions of the exposure, and the wind climate of the region. This is more so the case than simply increasing the size of members after accounting for lateral forces (Sharma et al., 2018; Jafari & Alipour., 2021). Near the ground, surface roughness reduces mean velocity, and the mean speed generally increases with elevation.

A. Problem Definition and Research Objectives

The analytical building in question is a 75 m tall, 25-storey reinforced concrete tower with nominal plan dimensions of 30m x 30m. The following five forms will be analyzed: a sharp corner square form, a recessed corner form, a chamfered corner form, a rounded corner form, and an optimized octagonal form. The estimated configurations have closely spaced fundamental periods, from approximately 1.736 s to 1.777 s. Hence, the configurations maintained a similar dynamic character while allowing for the corner treatments to be studied in an aerodynamic fashion. Wind demand was analyzed for six basic wind speeds ranging from 33 m/s to 55 m/s, assuming Terrain Category 3 conditions.

The 47 m/s case found in the analytical records associated with the Delhi/Patna wind condition will be the primary detailed comparison case, with the other cases serving as a range of speeds to check sensitivity. Of interest is a form that maintains a positive outcome throughout the wind speed range as opposed to a form that is advantageous only at a single, isolated condition. The software will be used to analyze diaphragm behavior and extract quantities such as fundamental period, base reactions, overturning moments, displacements, and drift, where lateral actions will be modeled as specified.

The main issue this work aims to solve is the lack of a clear, direct comparison of a few representative examples of corner treatments within one uniform ETABS model for a tall building. This lack of comparison makes it very hard to incorporate the results of aerodynamic studies into routine structural modeling using commonly found engineering software (Bernardini et al., 2015; Alkhatib et al., 2022).

B. Research Questions and Contributions

1) RQ1: How increasing basic wind speed affects the magnitude of structural response across the five configurations?
2) RQ2: Which corner treatment produces the greatest reduction in global force, represented primarily by base shear and overturning moment?
3) RQ3: Which treatment provides the lowest top displacement and inter-storey drift?
4) RQ4: Whether aerodynamic benefits remain consistent over the height of the tower or vary substantially between lower, middle and upper storeys?

©IJRASET: All Rights are Reserved

5) RQ5: Whether the optimized form maintains its relative advantage across the complete wind-speed range rather than only at the 47 m/s condition?

The main contribution of this work is not to say that a corner ratio is best in all cases, but to provide an engineering judgment on which of the considered options performs best for a 75 m building under the given assumptions, and to say what additional work would be needed to verify this for a given case in practice.

II. RELATED WORK

A. *Wind Loading, Dynamic Response and Serviceability of Tall Buildings*

Wind loading on tall buildings starts with the atmospheric boundary layer, where the roughness of the ground influences the speed and turbulence of the air. Generally, the mean velocity decreases as one goes down, and increases with height. Turbulence causes irregular fluctuations around the mean. Tanios (2016) describes how the mean velocity increases with height and distinguishes the mean and turbulent components of wind. Tanios (2016) says that the effect of a gust depends on the rate at which the wind changes, and the response of the building. The along wind response is caused by mean drag and turbulence. The force acts in the direction of the mean wind, and the mean value can be considered using an equivalent static method if the code requirements are met. The fluctuating value can cause the building to vibrate and increase the forces acting on the building.

Across-wind response is caused by pressure differences that are normal to the flow direction, and can be caused by many phenomena including vortex shedding and wake organization. For thin buildings, across-wind motion can be greater than along-wind motion, even if the building's plan area remains the same. This is because, for thin buildings, the flow interaction along the building can create an excitation force (Bezabeh et al., 2020; Wu, 2019). The third main type of response is torsional response. This type of response occurs when the aerodynamic loading is not centered about the building's (structure's) center of resistance, or if the pressure act on the opposite sides of the building are not equal. Even for a regular tower, modifying the corners can change the local pressures and the location of the resultant aerodynamic force. A complete evaluation of wind effects on buildings considers not only motion in two horizontal directions, but also rotation about the vertical axis. This numerical study focuses on global and storey translational responses. The available literature justifies the need for torsional responses in a full project model.

Rather than assessing only if a structure meets a single required wind case, the incorporation of performance-based techniques allows us to assess a range of wind cases, a range of potential responses, and the consequences of those responses. Bezabeh et al. (2020) take this broad approach to wind performance, while Cui and Caracoglia (2020) link wind performance to life-cycle impacts. Deng et al. (2019) also take a performance-based approach to wind resistance. In this study, the relative ranking of aerodynamic forms was assessed for the six specified wind speeds. It was hoped that this approach would provide a more manageable framework within which the negative consequences of increasing wind speeds could be evaluated. Full-scale monitoring also helps to interpret the dynamic performance of buildings under wind (Wu, 2019). The literature supports the view that responding to wind loads through strengthening of the structure is only one of many options.

B. *Aerodynamic Modification Strategies for Tall Buildings*

Aerodynamic modifications attempt to improve wind performance by altering the geometry that controls separation, pressure recovery, and the formation of wake. The literature tends to categorize these modifications as either major or minor strategies. Modifications that fall within the major strategy category transform the overall massing by tapering, setbacks, twisting, openings, varying plan dimensions, or by combining several forms over height. Modifications within the minor strategy category keep the main building envelope and transform corners and edges by recessing, chamfering, rounding, slots, fins, or other similar details. Both major and minor strategies are based on the same physical principle; the external shape of the building influences the distribution and coalescence of aerodynamic pressures, and a beneficial shape can reduce the load on the building structure (Sharma et al., 2018; Mooneghi & Kargarmoakhar, 2016). Of all the major strategies, tapering is perhaps the most well-known as it alters the width of the building over its height. Setbacks achieve a similar end result to tapering by disrupting the vertical correlation of vortex shedding. Like tapering, setbacks transform the effective aerodynamic scale seen by the wind. In setbacks, the plan is moved in an abrupt fashion, and as a result, the coherent wake is transformed at multiple elevations.

According to Li et al. (2018) and Li et al. (2020), the treatment of building corners can significantly change the wind loads acting on a hypothetical square super-tall building. One of the major advantages of such modifications is that to change a large part of the flow, a small change can be made in the building's geometry. The main objective is to modify the flow in such a way that vortex shedding is not organized. A square building corner has a sharp edge, and flow separation is fixed, and shear layers, which can couple to produce pressure differences, are formed.

If the edge is rounded, the separation location is moved, and the flow becomes curved, and pressure can recover along the path. The result is a narrow and possibly incoherent wake. Tse et al. (2021) also support the need for facade checks at later stages of the design, as corner changes relate to local wall pressures and global wind loads.

Wind loads must be integrated with the natural frequencies of the structure to determine if the structure will resonate. If damping is low, aerodynamic forces can easily excite a structure to vibrate. Changing the structure to alter the wake can also change the dominant shedding frequency or can serve to redirect the shedding to a broader range of frequencies. This is especially helpful in flexible towers, where changing the structure to achieve the needed stiffness would require a large amount of material. Jafari and Alipour (2021) support that shape modifications can be used in conjunction with other methods to mitigate vibrations, such as damping and stiffness. Many the published papers evaluate corner ratios in the range of 5 to 20 percent of a characteristic plan dimension.

From an aerodynamic perspective, maintaining spanwise coherence is important. Studies of U- and V-shaped or otherwise irregular plans likewise demonstrate the sensitivity of aerodynamic behavior to plan geometry (Mandal et al., 2021; Bhattacharya & Dalui, 2022; Mandal et al., 2022; Daemei et al., 2019). Tamura et al. (2017) highlight the impact of super-tall buildings on both the aerodynamics of the built environment and the wind experienced at the pedestrian level. Improving the structural response of a building may alter the downwash and recirculation near the ground. Xu et al. (2017) demonstrate that the built environments adapted for super-tall buildings may also alter the wind experienced at the pedestrian level, indicating that the built environment should be designed in an integrated manner to consider the public realm. Corner modifications can also influence the surrounding urban wind environment (Juan et al., 2024). There is a shift toward integrating geometry, structure, and response control devices in design to to better control the overall system.

C. Corner Modification: Sharp, Recessed, Chamfered, Rounded and Optimized Forms

Modifying corners on squares and rectangles is particularly effective for tall buildings, because the leading edges dictate where the flow adjacent to the façade separates. Sharp corners create separation and side-face suction that are fixed, and the detached shear layers swirl and mix in an unsteady flow in the wake. By modifying corners, designers can change this separation process without having to modify the entire building. Numerous tests, both from wind tunnels and computational analyses, show that a rounded, chamfered, or retracted corner can decrease the aerodynamic coefficients and the response induced by the wind, and can be effective in mitigating the problems caused by flow separation, although the impact is dependent on the geometry, the direction of the wind, and the turbulence in the fluid (Li et al., 2019; Li et al., 2023; Sanyal & Dalui, 2020). Corner recessions are obtained by removing or indenting a portion of the plan adjacent to the edge.

Li et al. (2020), in their studies using CAARC-type models, have shown that the aerodynamic performance is significantly influenced by the chamfer geometry. The analytical calibration shows that the chamfered form creates stronger reductions than the recessed form at the principal 47 m/s condition. Alminhana et al. (2018) and Li et al. (2018) support this rounded configuration and show that making changes to the standard tall-building models improves the pressure fields and aerodynamic coefficients. Al-Masoodi et al. (2023) support this view with their computational analysis. In their study, an octagonal configuration of a tall building was optimized, and a reduction in overall wind load of 31.67 percent, a 24.89 percent reduction in top deflection, and a 24.18 percent reduction in drift were reported. These findings support the reduction targets set for the optimized configuration in the analytical comparison. It is relevant to note that the structural response factors are supported by an aerodynamic optimization result, rather than being arbitrary. Surrogate models and multi-objective algorithms can help find the best modification ratios in a more reasonable time frame when compared to manual trials and errors (Elshaer et al., 2017; Lu et al., 2024). There are limitations to all of the methods mentioned. Results from wind tunnels depend on the scale, the type of boundary layer simulations, the instrumentation and the level of similarity.

D. CFD, Wind-Tunnel Testing and Computational Aerodynamic Optimization

Wind-tunnel testing and computational fluid dynamics (CFD) are the primary methods for simulating the impacts of wind on the design of tall buildings. Boundary-layer wind tunnels are used to create a vertical mean-velocity profile in the atmospheric flow along with turbulence and other length scales of interest. Rigid models can be instrumented to measure pressure coefficients or can be used in a force-balance framework. Aeroelastic models can be used to simulate motion if mass, stiffness, and damping are represented correctly. Wind tunnels are valuable because they can measure the integrated result of separated flow, and do not require the turbulence to be modeled numerically (Thordal et al., 2019). Blocken (2015) mentions that dependable CFD analyses require judicious choices of the computational domain, inlet profiles, boundary conditions, grid resolution, and numerical methods,

as well as adequate verification. Thordal et al. (2019) state that for the evaluation of CFD simulations of high-rise wind-loading, computational complexity is not the only metric; the represented physical quantities must also be correct. Increasing computational complexity to realize physical objectives can also be seen in the geometry-specific optimization of aerodynamic variables. Bernardini et al. (2015) provide a civil engineering case study using Kriging for aerodynamic shape optimization. Kriging provides an estimate of the response surface and probabilistic bounds, which allows the search algorithm to strike a balance between the uncertainty of the design space and the expected performance of the design. Alkhatib et al. (2022) use computational aerodynamic optimization to set performance criteria for geometric search in wind sensitive irregular tall buildings. In the process, they demonstrate that the aerodynamic role of CFD or wind-tunnel testing can be separated from the structural role of ETABS. ETABS, along with certain assumptions, can calculate the response of the structure. It cannot calculate the external flow around the building. A precise workflow can transform geometry-sensitive pressure fields from CFD or wind tunnel analyses into load patterns or equivalent storey forces, which can then be evaluated for displacements, drift, base shear, and overturning moments in ETABS.

III. METHODOLOGY

A. Overall Research Methodology

This study employed a quantitative, controlled comparison of wind-induced responses for five corner configurations of a reinforced-concrete building. The reference form M1 is a sharp-cornered square; M2, M3, M4 and M5 represent recessed, chamfered, rounded and octagonal corner treatments. Each form retains a nominal 30 m × 30 m footprint, 25 storeys of 3.0 m, an overall height of 75 m, M40 concrete and Fe500 reinforcement. The procedure first identifies the wind-speed and terrain assumptions, then calculates wind pressure at each floor-strip centroid, integrates the equivalent lateral actions over the height, and evaluates the response using a fixed-base linear-elastic cantilever idealization. The five forms differ by their prescribed force coefficients and effective flexural-rigidity multipliers. Structural consistency is therefore evaluated against explicit input assumptions rather than inferred from an undocumented ETABS model. This comparison offers a preliminary assessment of potential aerodynamic benefits, consistent with the broader rationale for corner treatment in tall-building studies (Bernardini et al., 2015; Alkhatib et al., 2022).

Six basic wind speeds, 33, 39, 44, 47, 50 and 55 m/s, are examined under Terrain Category 3. The 47 m/s condition, designated W4 (Delhi/Patna), is the principal comparison. At the 75 m roof, the interpolated terrain factor is $k_2 = 1.160$, giving $V_z = 54.520$ m/s and $p_z = 1.783$ kPa for W4 when $k_1 = k_3 = k_4 = 1.0$. Pressures acting on each of the 25 three-metre-high façade strips are evaluated at their mid-heights instead of uniformly applying roof pressure over the elevation. The corresponding lateral-force contributions are integrated to obtain base shear and overturning moment.

Roof displacement and inter-storey drift follow from the cantilever influence formulation, while an approximate first-mode period follows from the equivalent mass and flexural rigidity. These quantities are suitable for assessing relative trends but are not independent ETABS exports or final design-check results.

The analysis covers 30 wind–form combinations (five corner forms and six wind conditions), together with 125 storey-response records at W4 (25 storeys for each form). The reference value for each response is the M1 result under the same wind case; reductions are calculated separately for base shear, roof displacement and peak drift. Checks include monotonically increasing pressure and global action with wind speed, agreement between the sum of floor actions and base shear, agreement between floor-action moments and base overturning, correspondence between the roof row and global displacement, and correct drift calculation from consecutive floor displacements. A 2% damping ratio is retained as a structural input, but the equivalent-static cantilever calculations do not explicitly model dynamic damping, across-wind resonance or vortex-induced motion. Consequently, any subsequent detailed ETABS verification requires member properties, mass sources, diaphragms, supports, code load combinations and validated geometry-specific wind inputs.

B. Building Geometry, Material Properties and Structural Assumptions

The building examined in this work is a 25-storey reinforced-concrete tower with 3.0 m floor-to-floor height and a total structural height of 75 m. Its nominal plan dimensions are 30 m × 30 m, giving a height-to-width ratio H/B of 2.5. The same overall dimensions, windward façade width and floor-strip height are maintained across the five corner arrangements. Concrete grade M40 and reinforcement grade Fe500 establish a consistent material basis. For the elastic response comparison, the reference form is assigned an equivalent bending stiffness $EI = 8.20 \times 10^9$ kN·m² and a floor gravity/seismic weight intensity of 8 kN/m². These are idealized analysis inputs; they do not substitute for member-by-member sections or a verified ETABS mass and stiffness model.

Lateral response depends on the distribution of mass and stiffness through the building, diaphragm action, cracked-section properties and foundation restraints.

ISSN: 2321-9653; IC Value: 45.98; SJ Impact Factor: 7.538
Volume 14 Issue XI Nov 2026- Available at www.ijraset.com

The calculation therefore holds the same equivalent loading and support idealization for each geometric alternative, while applying documented form-specific EI multipliers of 1.000, 0.982, 0.972, 0.975 and 0.955 for M1–M5. On the associated uniform-mass cantilever basis, the approximate first-mode periods are 1.736, 1.752, 1.761, 1.759 and 1.777 s, respectively. The 2% damping assumption is a reporting parameter, not a modifier of these static deflections. Such a distinction is necessary because the listed periods are estimates from idealized elastic stiffness and mass rather than confirmed results of a three-dimensional ETABS modal analysis (Tanios, 2016).

TABLE I
BUILDING AND STRUCTURAL INPUTS USED FOR COMPARATIVE ANALYSIS

Model	Building form	Corner (%)	Width (m)	Storeys	Height (m)	T1 (s)
M1	Square (sharp corners)	0	30	25	75	1.736
M2	Recessed corners	7.5	30	25	75	1.752
M3	Chamfered corners	7.5	30	25	75	1.761
M4	Rounded corners	10	30	25	75	1.759
M5	Optimized octagonal corners	12	30	25	75	1.777

With H = 75 m, B = 30 m and a storey height of 3.0 m, the building has an aspect ratio of 2.5. The controlled geometric comparison therefore concerns a multi-storey building of moderate slenderness, not a super-tall building. The roof-height terrain adjustment and global moment arms are correspondingly based on 75 m and the individual floor-strip centroids.

In the context of ETABS, fixing material labels is critical to the consistency of the structural model. In addition to fixing material labels, geometry of beams, columns, walls and cores and thickness of slabs should be fixed based on the baseline model, and any changes in geometry should be documented. There should be geometric consistency in the assumptions of diaphragms, support conditions and mesh size. Drift and relative displacements are influenced by stiffness and distribution of loads, and a reasonable range of these parameters are reported for M1 to M5. It is expected that comparison of drift or relative displacements among different models should be influenced predominately by the intended aerodynamic variables and not by other design variables. It is summarized in Table I.

C. Aerodynamic Variants and Parameterization

The reference configuration M1 is a 30 m × 30 m square with sharp right-angled corners. The alternative designs are M2 with 7.5% recesses, M3 with 7.5% chamfers, M4 with 10% rounded corners and M5 with a 12% octagonal corner treatment. With the plan width B = 30 m, these dimensionless treatments correspond to nominal characteristic corner dimensions of 2.25 m, 2.25 m, 3.00 m and 3.60 m, respectively, subject to the geometric convention of each treatment. The five alternatives are compared with the same nominal windward width and the same 25-storey vertical arrangement. The modification percentage alone does not uniquely establish a buildable plan: recess depth, chamfer geometry, curve radius and octagonal vertices must be defined in construction drawings prior to any three-dimensional ETABS modeling.

Corner treatment is represented in this preliminary response calculation by an assumed equivalent force coefficient Cf and a form-specific stiffness multiplier, with the square reference assigned Cf = 1.300 and EI factor = 1.000. The corresponding values are M2: 1.178 and 0.982; M3: 1.105 and 0.972; M4: 1.118 and 0.975; and M5: 1.045 and 0.955. At a fixed wind condition the ratio of base shear to that of M1 is Cf/1.300; the relative displacement and drift factor is (Cf/1.300)/(EI factor) under the linear cantilever assumption. This explicit distinction avoids assigning unrelated reduction factors to force, displacement and drift. The coefficients are preliminary comparative assumptions, not independently determined pressure coefficients from wind-tunnel testing or a CFD solution, and must be validated before any project design use (Elshaer et al., 2017; Al-Masoodi et al., 2023).

©IJRASET: All Rights are Reserved | SJ Impact Factor 7.538 | ISRA Journal Impact Factor 7.894 |

TABLE III
AERODYNAMIC MODEL FACTORS USED IN THE COMPARATIVE ANALYSIS

Model	Building form	Corner (%)	Width (m)	Storeys	Height (m)
M1	Square (sharp corners)	0.0	1.300	1.000	1.0000
M2	Recessed corners	7.5	1.178	0.982	0.9228
M3	Chamfered corners	7.5	1.105	0.972	0.8745
M4	Rounded corners	10.0	1.118	0.975	0.8821
M5	Optimized octagonal corners	12.0	1.045	0.955	0.8417

Parameterization allows us to define and apply corner modifications consistently. Percent modifications should be defined based on a characteristic dimension. Consequently, each alternative should define a reference dimension to enable comparison of treatments such as 7.5, 10 and 12 percent modifications. Modifications of corners (by any given amount) can be expressed as either cut (or removal) of a portion of the corner, or by setting back a corner. The amount of setback represents the radius of a rounded corner. For the octagonal corners, each alternative should define the extent of the additional faces.

The windward façade strip width is held at 30 m in this calculation, while the corner coefficient distinguishes the five forms. For the same wind speed, coefficient ratios predict the relative base shears; the EI multipliers also influence periods, displacements and drift. Because all five forms are represented using a common simple beam idealization, the results isolate the assumed changes in overall loading and effective stiffness. They do not resolve local pressure concentrations, torsional effects, changes in plan area or Reynolds-number sensitivity. These limitations delimit the interpretation of the favorable ranking and define the need for detailed geometry-specific verification.

D. Wind Loading Model Based on IS 875 (Part 3):2015 Inputs

Wind loads are estimated with the velocity-pressure relationships in IS 875 (Part 3):2015. At elevation z, the design wind speed is $Vz(z) = Vb\ k_1\ k_2(z)\ k_3\ k_4$, and the corresponding nominal pressure in kPa is $pz(z) = 0.6\ Vz(z)^2/1000$. The adopted factors are $k_1 = k_3 = k_4 = 1.0$, with $k_2(z)$ interpolated between the listed Terrain Category 3 height values. In particular, $k_2(75\ m) = 1.160$, for the adopted 75 m roof. For each floor i, at centroid elevation $zi = (i - 0.5) \times 3.0$ m, the lateral action is $Fi = pz(zi) \times 30\ m \times 3.0\ m \times Cf$. At the 47 m/s case, roof pressure is 1.783 kPa and roof speed is 54.520 m/s. Calculating floor actions at centroid heights accounts for variation of wind intensity over the building. Site-specific exposure, dynamic/gust procedures, wind direction, pressure coefficients and other code conditions remain necessary for final engineering design.

$$V_z = V_b \times k_1 \times k_2 \times k_3 \times k_4$$

$$p_z = 0.6 \times V_z^2$$

TABLE IIIII
WIND CASES USED FOR THE AERODYNAMIC COMPARISON

Wind ID	Representative City / Zone	Vb (m/s)	k_2 at 75 m	Vz (m/s)	pz (kPa)
W1	Bengaluru	33	1.160	38.280	0.879
W2	Ahmedabad	39	1.160	45.240	1.228
W3	Mumbai / Hyderabad	44	1.160	51.040	1.563
W4	Delhi / Patna	47	1.160	54.520	1.783
W5	Chennai / Kolkata	50	1.160	58.000	2.018
W6	Darbhanga	55	1.160	63.800	2.442

The six wind cases are of special interest because they illustrate how wind velocity relates to pressure and how that relationship can vary. Wind speed and pressure are related such that a change in wind speed (in this case an increase from wind case 1 to wind case 6) does not affect pressure in a linear fashion.

©IJRASET: All Rights are Reserved | SJ Impact Factor 7.538 | ISRA Journal Impact Factor 7.894 |

Rather, the relationship is squared. Because of this, the increase in pressure from wind case 1 to wind case 6 is disproportionately larger than the increase from basic wind speed 1 to basic wind speed 6. The analysis should be checked by ensuring that the relationship between pressure and the corresponding response (e.g. deflection, stress, etc.) is reasonable. Departure from this should prompt a review of the analysis.

It should be stressed that the use of the design wind coefficients described in this report is to be considered part of a comparative case scenario and should not be considered a complete evaluation of the project. Many variables that affect the determination of the critical design wind case (e.g. risk and exposure, terrain and nearby obstructions, land use, etc.) will vary from project to project and would need to be analyzed to define the critical design wind case for a project. The intent of this report is to analyze the effects of corner case geometry of a building in a constant or uniform environment (e.g. wind case 1 to wind case 6).

E. ETABS Analysis Settings, Load Cases and Response Extraction

The 25-storey model is represented for this comparative analysis by a fixed-base equivalent linear-elastic cantilever. A 30 m × 30 m nominal plan, 3.0 m storey interval, common floor weight intensity and a reference flexural rigidity are assigned. For each wind case, the height-varying terrain coefficient gives the pressure at 25 floor-strip centroids. The product of pressure, 90 m² strip area and each form's Cf gives a floor-level horizontal force; summation provides base shear, and summing force times centroid elevation provides overturning moment. A cantilever influence kernel and the selected effective EI produce floor displacement, roof displacement and drift. The approximate first-mode period is obtained from the analytical cantilever frequency relationship. In contrast, an ETABS implementation would require explicit beams, columns, walls, diaphragms, mass source, section stiffness, load patterns and analysis controls. The present numerical results should not be labeled as exported ETABS results until such an implementation has been carried out and independently checked.

TABLE IVV
ETABS MODELLING, ANALYSIS AND OUTPUT PROTOCOL

Stage	Required Action	Key Evidence
Geometry	Define 25 storeys, grids and member layout	3D model and plan/elevation views
Materials/sections	Assign M40, Fe500 and member properties	Property-definition tables
Mass/diaphragms	Define mass source and floor diaphragm behavior	Mass-source and diaphragm settings
Wind cases	Create consistent wind actions for all alternatives	Load-pattern and case definitions
Dynamics	Estimate cantilever period; check 2% dynamic damping in later ETABS analysis	Periods and mass participation
Second order	Check P-Delta in subsequent detailed structural model	Analysis-option record
Results	Export reactions, drift, displacement and storey shear	Calculated floor-force and response tables; ETABS verification pending

For subsequent ETABS implementation, all five 25-storey forms should adopt the same gravity loading basis, material specifications, modeling conventions and control elevations. The 2% damping value is relevant to dynamic response analysis, but does not affect the static cantilever calculations reported here. Modal mass participation, torsional periods, P-Delta effects, support conditions and code load combinations must be checked directly in the structural software. Agreement between an eventual ETABS result and the screening calculation should be verified, not assumed.

Response alternatives should be defined consistently. Base shear should be taken from reactions of the same support. Overturning moments should be taken from the same reference level. Displacements should be taken from the same control points or diaphragms. For each model, the direction of greatest response should be identified and unambiguously referenced. If response in each storey is reported, consistency should be ensured in the reference storey and units. These standards should be established prior to comparison of the models.

F. Data Analysis, Reduction Metrics and Visualization Procedure

For a given wind case, each response reduction is computed as Reduction (%) = [(R_M1 − R_Mi)/R_M1] × 100, where R_M1 is the baseline value and R_Mi is the value for a modified form. Parentheses are essential to calculate the percentage correctly. At W4, the evaluation covers the base shear, base overturning moment, roof displacement and maximum inter-storey drift ratio of all five forms. Since wind pressure varies as V_b^2 when the other coefficients are fixed, the six-case comparisons provide a direct check of proportional load sensitivity. For the elastic cantilever formulation, roof displacement and drift scale with Cf/EI and the common wind force profile. Normalized reductions and the height-to-roof-displacement ratio H/Δ are calculated using the same building height, H = 75,000 mm, throughout.

$$\text{Reduction (\%)} = \left[\frac{R_{\text{baseline}} - R_{\text{modified}}}{R_{\text{baseline}}}\right] \times 100$$

Storey-wise displacement, drift and shear are examined at W4 over 25 storeys in each of the five alternatives, producing 125 records. The elevation of floor i is 3i metres. Inter-storey drift is defined as Δi = ui − ui−1, where u0 = 0 at the base; the drift ratio is Δi/3000 mm. Storey shear at floor i is the sum of the lateral actions applied at that floor and all higher floors. Thus cumulative shear decreases with elevation, whereas the integrated cantilever displacement rises towards the roof. The response profiles also provide internal checks: the uppermost recorded displacement must equal the global roof displacement, the maximum derived drift ratio must reproduce the global value, and the lowest cumulative storey shear must equal the base shear.

Design wind pressure is reported to three decimals, approximate modal period to three decimals, forces and displacements to a suitable level of engineering precision, and percentage savings to two decimals. Full-precision values are retained in the calculations. These rounded outputs must not be mistaken for structural design capacities or compliance statements. The ranking considers base shear, overturning moment, roof displacement and peak drift, with each metric evaluated at the same wind speed. The six-case comparison tests stability of that ranking; it does not account for different angles of incidence or gust-response amplification. This interpretation is consistent with multi-criterion aerodynamic assessment, in which force reductions alone do not establish all aspects of building performance (Bernardini et al., 2015; Al-Masoodi et al., 2023).

IV. MODELLING AND ETABS IMPLEMENTATION

A. Baseline ETABS Model Development

A 25-storey square-plan building defines the reference form M1, with 3 m storey height, total height 75 m and 30 m × 30 m nominal plan dimensions. The present calculations describe its response through a fixed-base equivalent cantilever of EI = 8.20 × 10^9 kN·m², with M40 concrete and Fe500 reinforcement identified as the common material assumptions. Wind pressure is applied through 25 lateral strip forces in each wind case. A detailed ETABS model would require physically defined beams, columns, walls, floor slabs, rigid or semi-rigid diaphragms, a documented mass source and appropriate cracked-stiffness modifiers. Consequently, the present numerical comparison provides a preliminary structural response benchmark rather than evidence that a complete 25-storey ETABS model has already been assembled and checked.

The baseline is the common reference for all corner alternatives. Its basic wind pressure is integrated floor by floor, and the resulting cantilever forces and deflections establish the denominator for response-reduction calculations. To implement the same design in ETABS, consistent geometry and gravity loads must first be confirmed. Subsequent plan modifications should not unintentionally change slab area, mass or the assumed lateral system without documenting the effect.

There are a number of dynamic checks that should also be performed. The period of the first mode of vibration should be within the expected range, and the principal modes of vibration should resemble reasonable shapes for a building of this type. The mass ratios should be reviewed before other checks are performed. Wind responses and other checks are performed relative to the baseline model; therefore, it is important that the baseline model be accurately represented. It is good practice to capture the settings and results of comparisons with the baseline case to ensure that any reductions in model performance are not the result of unforeseen changes to the structural model.

B. Implementation of Aerodynamic Modified Models

The modified configurations M2–M5 retain 25 storeys, 75 m height and a 30 m nominal plan width. Recessed, chamfered, rounded and octagonal corners are distinguished by the specified treatment ratios and force coefficients. Their assumed Cf values are 1.178, 1.105, 1.118 and 1.045, respectively, compared with 1.300 for M1. Their effective EI factors, relative to the square reference, are 0.982, 0.972, 0.975 and 0.955.

A decrease in loading may offset a modest decrease in effective stiffness, so both inputs are needed when discussing displacement or drift. A detailed ETABS comparison would require precise corner coordinates and a documented structural redistribution around the altered perimeter.

Geometric percentages are found in plans and coordinate tables. Thesepercentages are referenced relative to plan dimensions. These dimensions are referenced to plan corners. The percentage may be based on plan width. When this is the case, the dimensional values for rounded corners or setbacks need to be specified to indicate the treatment. This is especially true when comparing results from aerodynamic studies. Corner treatment affects flow separation and reattachment and hence the aerodynamic performance of the model. Geometric consistency is critical for attributing differences in structural response to aerodynamic performance. Variations in corner dimensions and treatments may influence wind-induced forces and the corresponding structural response.

Both paths of analysis are valid. In the first case, the plan floors are shaped as desired in ETABS. In this case, the floor shape may influence changes in mass, stiffness, and other properties. Isolating effects requires that the changes caused by shaping floors be accounted for. In the second case, the plan is shaped as a square, and the other sides of the plan are shaped as desired. In this case, the effects of treatment are attributed strictly to aerodynamic loading.

C. Wind Load Cases, Combinations, Modal Analysis and P-Delta

For W1–W6, the basic wind speeds range from 33 to 55 m/s. Design wind speed is calculated at the centroid of each of the 25 floor strips using the Terrain Category 3 height factor, and pressure follows $pz = 0.6Vz^2/1000$ in kPa. Under the W4 case, the 75 m roof speed is 54.520 m/s and the roof pressure is 1.783 kPa. Storey forces are formed from each strip's pressure, 30 m width, 3 m height and the adopted corner coefficient. Base shear and overturning moment are then integrated from these actions. ETABS wind-pattern definition and appropriate pressure/load cases remain independent verification tasks rather than a calculation already completed in this study.

For subsequent finite-element analysis, equivalent wind-only results and the governing service and strength load combinations should be distinguished. ETABS load patterns and load-combination multipliers must be documented so that the reported response can be traced to a specific wind case. Modal analysis should consider sufficient eigenvector or Ritz modes to attain the participation required by the governing analysis method; the number of modes appropriate to another building cannot be assumed for this 25-storey structure. When a complete model is available, the analyst should verify horizontal mass participation, mode shapes and the relevance of the 2% damping assumption to the selected dynamic analysis (Tanios, 2016; Bezabeh et al., 2020). These steps are verification requirements and were not established by the equivalent-static beam analysis.

The estimated first-mode periods are M1 = 1.736 s, M2 = 1.752 s, M3 = 1.761 s, M4 = 1.759 s and M5 = 1.777 s. These values result from the fixed-base uniform-mass cantilever expression, $T1 = [2\pi/(1.875^2)]\sqrt{(mH^4/EI)}$, using H = 75 m and the specified effective flexural rigidities. The slightly longer periods of the modified forms follow their lower effective EI values; they are not the measured modal periods of ETABS models. A 2% damping ratio has been documented for subsequent dynamics but is not applied to the static wind deflection calculations. Verification of modal participation and wind-induced dynamic response remains necessary before these periods are used for final design.

D. Model Validation, Comparability and Sensitivity Checks

Three consistency checks support the numerical comparison. First, every form has 25 storeys, a 75 m height, a common 30 m windward width and the same wind-case factors. Second, total floor forces equal the reported base shears and their force–height products equal the overturning moments. Third, storey deflections, drift increments, peak drift ratios and global roof displacements agree in units and terminal values. These are arithmetic and mechanical consistency checks for an idealized analytical model, not proof of code compliance or an independently validated ETABS solution. The changing plan may also alter real stiffness and mass distributions beyond the single EI multiplier, which warrants separate structural verification.

Each alternative must be compared using consistent height, number of storeys, material assumptions, wind profile, loading units and equivalent support conditions. Within the present calculation, the same 25 floor levels and basic reference EI are defined, while the corner coefficients and prescribed EI multipliers vary. In a future three-dimensional model, additional checks must establish consistent diaphragm behavior, mass sources, member properties, support conditions and modal participation; these properties have not yet been verified from ETABS exports.

Reviews should evaluate which assumptions would cause the most change in the ratings. These assumptions may include the aerodynamic loading case, the direction of the wind, the damping of the structure, and the lateral-stiffness of the structure. The ratings may change based on slight changes in the assumptions.

©IJRASET: All Rights are Reserved | SJ Impact Factor 7.538 | ISRA Journal Impact Factor 7.894 |

If the assumptions are changed in a way that is likely to occur in practice, and the ratings of M2 with respect to M5 is the same, then we may have more confidence in the ratings. The comparison between M2 and M5 should therefore use a consistent reference and clearly state whether lower structural demand or greater reduction is preferred.

E. Detailed ETABS Modelling Parameters and Analysis Control

The equivalent structural system is a 25-storey, 75 m fixed-base cantilever with a 30 m × 30 m nominal plan, M40 concrete, Fe500 reinforcement, a floor-load intensity of 8 kN/m² and a reference stiffness EI = 8.20×10^9 kN·m². Each story occupies a 3 m vertical strip; wind loads are evaluated at the strip's mid-height. Equivalent flexural rigidity is reduced for the modified forms according to the specified EI multipliers, which are explicitly retained in the response calculations. This representation does not contain detailed beams, columns, shear walls or floor diaphragm elements; those properties are reserved for a subsequent three-dimensional structural model.

Before comparing the wind cases, the assumed fixed-base boundary condition, 25 floor elevations, force coefficients and equivalent stiffness factors were checked for consistency. Calculated base forces, moments, roof deflections and floor-to-floor drifts were compared across the global and storey records. Detailed verification of member releases, diaphragm connectivity, modal mass and higher vibration modes requires a three-dimensional ETABS model and is outside the completed analytical calculations.

TABLE V
DETAILED ETABS MODELLING PARAMETERS AND ANALYSIS CONTROLS

ETABS item	Common modelling requirement	Purpose in comparison
Geometry	25-storeys; 75 m height; 30 m × 30 m nominal plan; 3.0 m storey height	Keeps overall building scale constant
Materials	M40 concrete and Fe500 reinforcement	Avoids material-strength bias
Dynamic basis	2% damping; modal periods checked for each form	Confirms comparable dynamic behaviour
Diaphragms and mass	Same floor diaphragm and mass-source assumptions	Prevents artificial changes in lateral response
Wind loading	W1-W6; 33-55 m/s; W4 = 47 m/s principal case	Provides controlled demand and sensitivity checks
Response outputs	Base shear, OTM, roof displacement, drift, storey shear and modal period	Provides strength and serviceability evidence

F. ETABS Output Verification and Model Acceptance Checks

The calculations were checked for physical trends and numerical agreement. Over the six cases, the common velocity factors produce pressure proportional to Vb^2; the calculated base shear and overturning moment increase accordingly. The 25-floor displacement profiles rise smoothly from the restrained base to the roof, while cumulative storey shear reduces with elevation. Differences in lateral demand across forms follow the assumed coefficients and stiffness values. These tests identify inconsistencies in the computations but do not replace a finite-element model audit, dynamic wind assessment or code-design verification.

The global wind–form matrix contains 30 cases. Each case records the corner form, wind speed, roof-adjusted wind speed, roof pressure, base shear, overturning moment, approximate period, roof displacement, maximum drift and height-to-roof-displacement ratio. Storey response is reported for the five forms at W4, giving 25 records per form and 125 records in total. The base reaction values are derived from summed floor actions, not taken from a structural software reaction export. Distinct case identifiers prevent the results from different wind speeds or forms from being mixed when presenting the plots.

For every storey record, the floor level, top elevation, direct lateral force, cumulative shear, lateral displacement, inter-storey drift and drift ratio are retained. The floor-25 displacement must agree with the global roof response for that form; the largest drift must agree with the corresponding global drift value. The ratio H/Δ is calculated with H = 75,000 mm and Δ expressed in millimetres. Under W4, the base-shear saving of the octagonal form, for example, is $(4371.46 - 3513.98)/4371.46 \times 100 = 19.62\%$. This reproduces the arithmetic of the reported response and avoids an unsupported interpretation as an ETABS output.

Reproducibility is supported by the explicit wind factors, 25-level force integration, form coefficients and stiffness multipliers. The analysis should be recalculated if the storey count, overall height, material stiffness, lateral loading assumption or any corner factor changes. The graphical summaries use the same 30 global cases and the 125 storey records of W4. A subsequent ETABS comparison will additionally require the structural model file, exact corner coordinates, diaphragm definitions, solver options, load combinations and independently derived aerodynamic inputs; these are not established by the present cantilever results.

V. RESULTS AND DISCUSSION

A. Comparative Global Response at the 47 m/s Principal Wind Case

For the principal W4 condition, Vb = 47 m/s, the 75 m roof design wind speed is 54.520 m/s and the corresponding pressure is 1.783 kPa. The square reference M1 gives a base shear of 4,371.46 kN, overturning moment of 177,909.07 kN·m, roof displacement of 31.327 mm, peak inter-storey drift ratio of 0.000560 and approximate fundamental period of 1.736 s. These results arise from height-varying floor wind actions and the equivalent elastic cantilever model. They establish a consistent comparison with the four modified corner forms, rather than proving structural adequacy in a complete ETABS design (Elshaer et al., 2017; Li et al., 2020).

The recessed-corner M2 model develops a base shear of 3,961.22 kN, overturning moment of 161,212.99 kN·m, roof displacement of 28.907 mm and maximum drift ratio of 0.000517 under W4. Relative to the square form, these values represent a 9.38% reduction in base shear and overturning moment and a 7.72% reduction in roof displacement and peak drift. The reduced corner-force coefficient lowers wind action, while the 0.982 effective-stiffness factor partly offsets the corresponding displacement benefit. This result represents the assumed equivalent response to the recessed geometry and requires corroboration with pressure measurements or geometry-resolved flow modeling (Al-Masoodi et al., 2023).

For the 7.5% chamfered model M3, the W4 base shear is 3,715.74 kN and the overturning moment is 151,222.71 kN·m. The corresponding roof displacement is 27.395 mm and the peak drift ratio is 0.000490. The force reduction is 15.00%, whereas roof displacement and drift decrease by 12.55% after considering the EI factor of 0.972. Chamfering is thus the second-best configuration in the present set across these four criteria. Its assumed force coefficient is smaller than that of the recessed and rounded forms, consistent with the potential aerodynamic advantage of corner truncation reported in the literature (Li et al., 2020; Lu et al., 2023).

The 10% rounded-corner alternative M4 produces a W4 base shear of 3,759.46 kN, an overturning moment of 153,001.80 kN·m, roof displacement of 27.632 mm and maximum drift ratio of 0.000494. Relative savings are 14.00% in global force and moment and 11.79% in displacement and drift. These values are close to, but slightly less favorable than, the chamfered form. The response ordering is tied to the adopted force and rigidity factors; rounding does not invariably have an inferior aerodynamic effect because the actual separation behavior depends on corner radius, incident wind direction and local flow conditions.

The octagonal corner model M5 has the smallest equivalent response under W4: base shear 3,513.98 kN, overturning moment 143,011.52 kN·m, roof displacement 26.368 mm and maximum drift ratio 0.000471. Compared with the square model, the reductions are 19.62% in shear and moment and 15.83% in displacement and drift. The octagonal force coefficient of 1.045 is the smallest in the adopted set, despite its effective stiffness being reduced to 95.5% of the reference value. Thus, its loading advantage is sufficient to outweigh the assumed stiffness reduction. The finding is a conditional ranking for this controlled analysis, not a verified universal optimum or an independently measured wind-tunnel result (Al-Masoodi et al., 2023).

The approximate first-mode periods increase slightly from 1.736 s for M1 to 1.777 s for M5 because the adopted flexural rigidity decreases across the alternatives.

The intermediate periods are 1.752 s (M2), 1.761 s (M3) and 1.759 s (M4). A longer period does not establish better aerodynamic performance; the principal evidence for the form ranking is the reduction in applied equivalent wind action and in the associated elastic response.

The calculated periods describe the idealized beam representation and must be checked through three-dimensional modal analysis before drawing conclusions about resonance or occupant comfort.

The W4 response order is consistent for base shear, overturning moment, roof displacement and peak drift: M5 octagonal, M3 chamfered, M4 rounded, M2 recessed, followed by M1 square in descending order of benefit. This shared ranking occurs because the equivalent wind profile is common and the form coefficients are held constant for all floors; the displacement ranking also reflects the documented EI multipliers. The data do not establish fatigue resistance, connection capacities, local cladding pressures, across-wind response or code compliance. These issues remain independent checks for detailed structural design.

©IJRASET: All Rights are Reserved

TABLE VI
STRUCTURAL RESPONSE COMPARISON AT THE 47 M/S PRINCIPAL WIND CASE

Building form	Base shear (kN)	OTM (kN·m)	Top disp. (mm)	Max drift ratio	T1 (s)
M1 - Square	4,371.46	177,909.07	31.327	0.000560	1.736
M2 - Recessed	3,961.22	161,212.99	28.907	0.000517	1.752
M3 - Chamfered	3,715.74	151,222.71	27.395	0.000490	1.761
M4 - Rounded	3,759.46	153,001.80	27.632	0.000494	1.759
M5 - Optimized octagonal	3,513.98	143,011.52	26.368	0.000471	1.777

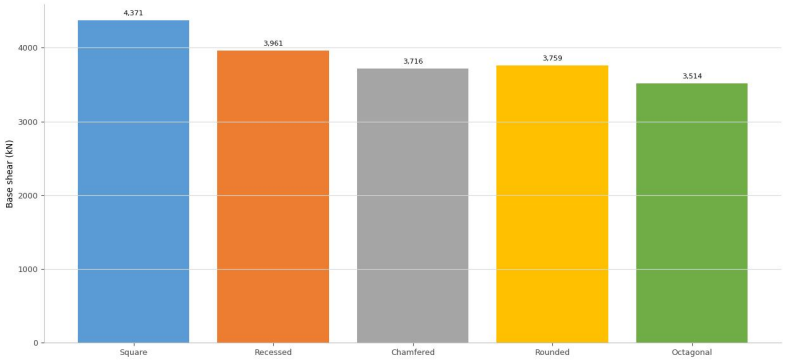


Fig. 1 Base Shear of the Five Building Forms at 47 m/s

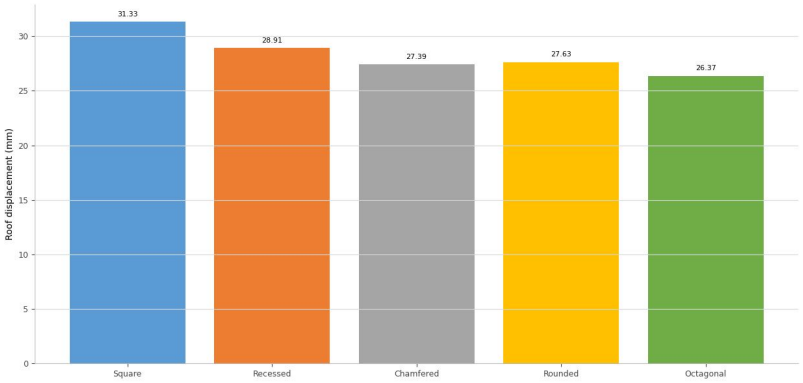


Fig. 2 Overturning Moment Relative to the Square Baseline at 47 m/s

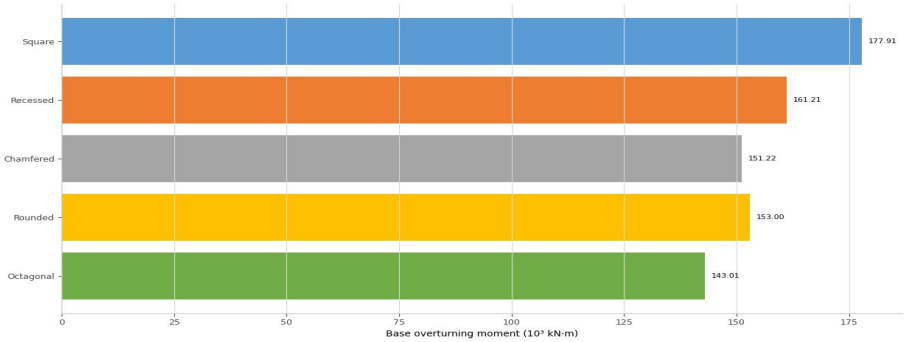


Fig. 3 Roof Displacement of the Five Building Forms at 47 m/s

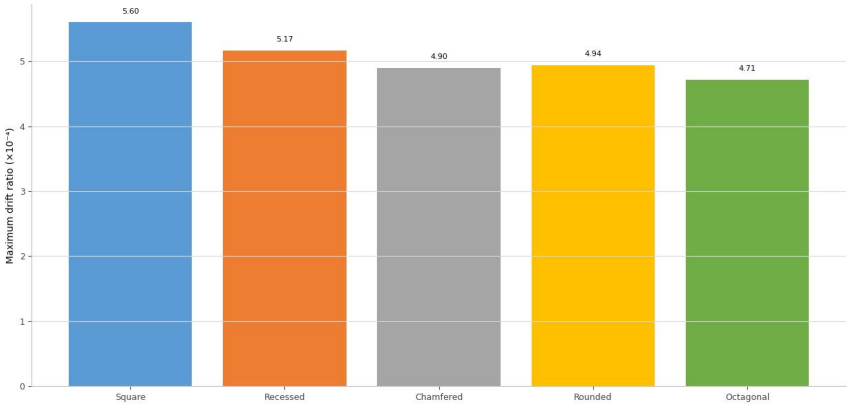


Fig. 4 Roof Displacement of the Five Building Forms at 47 m/s

The W4 comparison shows that each modified form reduces the computed base shear, overturning moment, roof displacement and peak drift ratio relative to the square reference. For M2–M5, the base-shear reductions are 9.38%, 15.00%, 14.00% and 19.62%, respectively, while the corresponding displacement and drift reductions are 7.72%, 12.55%, 11.79% and 15.83%. Lower force coefficients account for the global-force savings. The slightly smaller deformation savings are expected because each modified form also carries a lower assumed effective flexural stiffness than M1.

The chamfered and rounded options are close in calculated performance. M3 carries 3,715.74 kN of base shear and 27.395 mm of roof displacement, compared with 3,759.46 kN and 27.632 mm for M4. This difference should not be generalized without resolving the flow around the actual corner dimensions. At the screening stage, both forms provide a substantial improvement over the square case, but M3 retains the slightly more favorable normalized force-to-stiffness ratio.

B. Wind-Speed Sensitivity of Global Responses

Wind-speed sensitivity is assessed for all five configurations under W1–W6, from 33 to 55 m/s basic wind speed. The same terrain profile and form coefficients apply to each wind case, so the global response scales with the square of basic wind speed. For the square reference, base shear increases from 2,155.06 kN at 33 m/s to 5,986.27 kN at 55 m/s; for the octagonal form, the corresponding values are 1,732.34 and 4,812.04 kN. The comparison therefore tests a consistent load-intensity range rather than changing geometry or the model's material properties with wind speed.

For all six wind intensities, M5 retains the lowest base shear, followed by M3, M4 and M2, with M1 highest. The percentage base-shear reductions relative to M1 are constant across the six cases: 19.62% for M5, 15.00% for M3, 14.00% for M4 and 9.38% for M2. This stability is a direct consequence of maintaining fixed form coefficients, not evidence that the true aerodynamic coefficients remain invariant with Reynolds number, wind direction or turbulence intensity. Absolute benefits grow as wind speed increases because the horizontal forces depend on wind pressure.

The roof-displacement responses follow the same consistent ordering. At 33 m/s, the square and octagonal forms displace 15.443 mm and 12.999 mm, respectively; at 55 m/s the values rise to 42.899 mm and 36.109 mm. Across the same cases, the octagonal roof-displacement and drift reductions remain 15.83%, because the ratio of its force coefficient to effective stiffness is unchanged. These comparisons distinguish the absolute deformation demand, which rises strongly with speed, from the normalized shape benefit, which is held constant by the analytical assumptions.

The absolute base-shear saving of the octagonal form increases from 422.72 kN at 33 m/s to 1,174.23 kN at 55 m/s. The corresponding roof-displacement difference increases from 2.444 mm to 6.790 mm. Although larger wind intensity increases the potential benefit of reduced equivalent loading, these numbers alone do not justify reducing structural member sizes. Gravity demands, drift criteria, stability, strength, ductility and the controlling load combinations must all be checked in the detailed structural model.

The multiple design wind speeds analyzed in the sensitivity comparison also demonstrate the importance of evaluating more than one design wind speed. A basic case typically identifies the preferred structure shape at a given design wind speed. However, that case doesn't illustrate how the preferred shape would respond to variations in the wind speed and direction. The examples illustrated in this study demonstrate that, as the design wind speed increases, the shape that offers the best performance/response also becomes

preferable. This approach aligns with performance-based design by examining structural response to varying wind loads rather than relying solely on a single code-defined loading case. In this respect, it is suggested that, in the design of a tall building, a response surface be developed that defines the limits of the response of the building to varying wind conditions, as opposed to focusing on the results of a single wind case study.

However, wind-speed sensitivity alone does not provide a complete assessment of the analytical comparisons. Actual wind conditions include variability in direction, turbulence and gusts. Urban wind conditions are additionally affected by the layout and shape of surrounding buildings and the surface laid out over the ground. There may be along-wind and across-wind variability and interaction with other wind conditions. What is favorable in one approach may not be the case in other approaches. Wind effects not represented in these analytical comparisons may also influence building response. Actual wind conditions are unlikely to remain otherwise identical across the different wind-speed intensities considered. The wind conditions used to generate the wind-speed curves are intended to demonstrate the stability of the selected ranking at the six wind-speed conditions and not to demonstrate what may happen at other wind conditions. Lu et al. (2023) note that serviceability and survivability of buildings should be considered together, and particularly so in the case of buildings with dramatic and/or unusual shapes.

Within this 25-storey analytical comparison, the octagonal model remains the preferred form for all six basic wind speeds. The chamfered option ranks second, followed by rounded and recessed treatments. Because the same force coefficients and stiffness multipliers are applied at every speed, the unchanged ordering is a property of the stated assumptions. The design recommendation should therefore be tested by direction-sensitive CFD or wind-tunnel pressures and by a complete ETABS model before project selection.

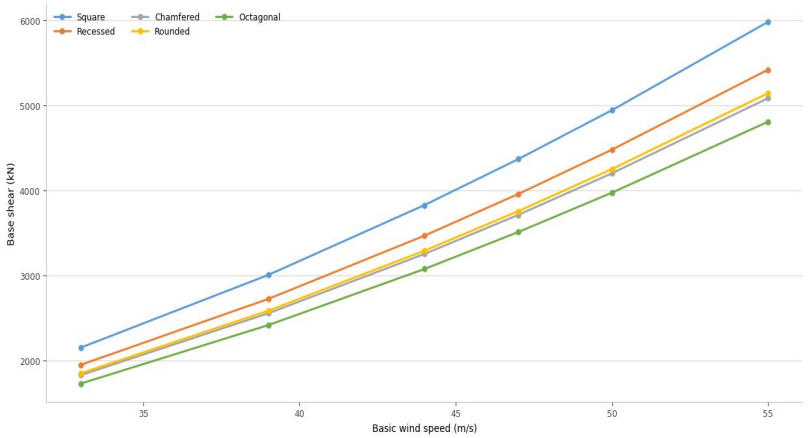


Fig. 5 Base Shear Sensitivity across Six Basic Wind Speeds

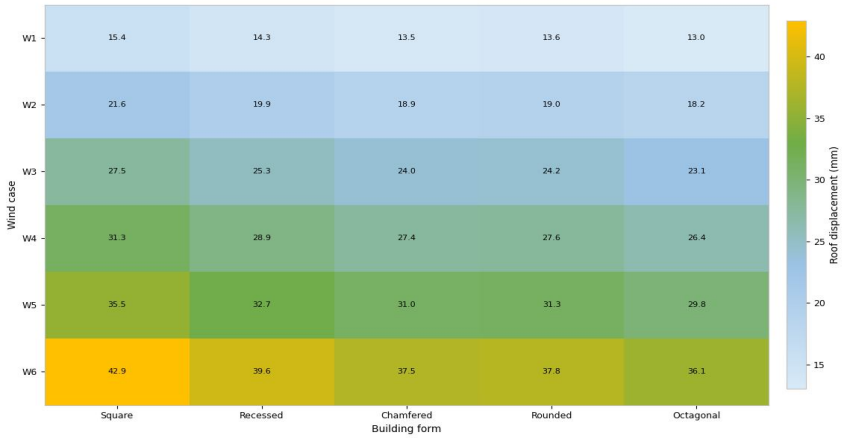


FIG. 6 Roof Displacement Heatmap by Wind Speed and Building Form

The sensitivity analysis considers the effect of more variable wind conditions, and takes into account a range of average wind speeds. For wind speeds up to 55 m/s, predicted design pressures increase significantly. Consequently, expected base shears and structure displacements also increase. It is important to determine whether modified wind models maintain their relative rank order with respect to base shear and displacement demand. If the rank order remains unchanged across the six wind-speed cases, the form with the lowest predicted structural demand retains the greatest comparative benefit under the adopted assumptions. Therefore, for wind speeds greater than the design condition, the treatment is expected to reduce the demand on the structure.

These concepts are more clearly illustrative for the case of the optimized octagonal model. For wind speeds less than the design condition, W4 in this case, it is expected that the model with the treatment would have the least demand. However, for wind speeds W5 and W6, it is expected that other models without the treatment would have greater demand. The sensitivity graphs facilitate identification of inconsistencies in the case model and input data. Other assumptions being constant, abrupt reversals in the graph are not justified and require adjustment. The analysis of wind speed demonstrates that, for the case models, the treatment is justified and that greater demand on the models is reasonable. It can also be concluded that for greater wind speeds the models without treatment are expected to have greater demand.

C. Storey-wise Displacement and Drift Behavior

The W4 storey-response profiles were calculated for all 25 floors of each form, using 3.0 m height intervals. Lateral displacement increases smoothly from the restrained base to the 75 m roof for every alternative. The square form has the largest top displacement, 31.327 mm, while the octagonal configuration has the smallest, 26.368 mm. Intermediate roof values are 28.907 mm for recesses, 27.395 mm for chamfers and 27.632 mm for rounding. The absence of abrupt changes in these idealized profiles supports the internal consistency of the cantilever calculation, but does not demonstrate that a detailed frame-and-core system has no local irregularities.

Near the base, all forms have relatively small lateral deflections because the equivalent cantilever is fully restrained at the foundation. Deflection differences increase gradually with height as bending deformation accumulates. The forms share the same horizontal load distribution with elevation, apart from their coefficient multipliers, and each has a form-specific effective EI. The profiles therefore have similar shapes but different magnitudes. This behavior is consistent with linear elastic flexure and should not be interpreted as a detailed examination of diaphragm flexibility or local storey stiffness variations.

Inter-storey drift is important for cladding, partitions and serviceability. At W4, the maximum ratios are 0.000560 for the square reference, 0.000517 for the recessed form, 0.000490 for the chamfered form, 0.000494 for the rounded form and 0.000471 for the octagonal form. For the octagonal treatment, the peak drift ratio is 15.83% below the square-model value; for the chamfered treatment the reduction is 12.55%. These quantities are computed from the differences between successive floor displacements divided by a 3,000 mm storey height.

The calculated absolute inter-storey drifts increase smoothly towards the upper floors, reaching maximum values of 1.680 mm, 1.550 mm, 1.469 mm, 1.481 mm and 1.414 mm for M1–M5, respectively. They do not display a soft-storey discontinuity because the simplified cantilever assumes uniform effective stiffness over height. Final checks on the actual structural design must therefore examine storey stiffness, member deformation, diaphragm interaction and second-order drift amplification independently.

A complementary deformation measure is H/Δ, where $H = 75{,}000$ mm and Δ denotes roof displacement in millimetres. At W4 the ratios are approximately 2,394 for the square, 2,595 for the recessed, 2,738 for the chamfered, 2,714 for the rounded and 2,844 for the octagonal form. A larger H/Δ denotes smaller roof displacement relative to building height under the stated load case. This ratio is a descriptive stiffness-response index, not by itself a code-prescribed acceptance limit.

Formal serviceability assessment requires the governing design combination, the actual member stiffness and the applicable project-specific displacement and drift limits. The values reported here are comparative elastic-response estimates only. The octagonal form has the lowest roof displacement and peak drift in the selected 47 m/s calculation, but its apparent benefit does not demonstrate resistance to other load types or establish acceptable occupant comfort, member strength or drift compliance. Such conclusions require independent structural and dynamic checks.

The close correspondence between relative roof-displacement and peak-drift improvements is expected for a uniform cantilever whose loading shapes do not change between forms. Both elastic responses scale with the equivalent lateral force coefficient divided by effective EI. Therefore, the same nominal 15.83% improvement is obtained for displacement and drift for the octagonal option, while its base-shear saving is 19.62%. The distinction arises from reduced effective stiffness of the corner-modified equivalent structural systems.

©IJRASET: All Rights are Reserved | SJ Impact Factor 7.538 | ISRA Journal Impact Factor 7.894 |

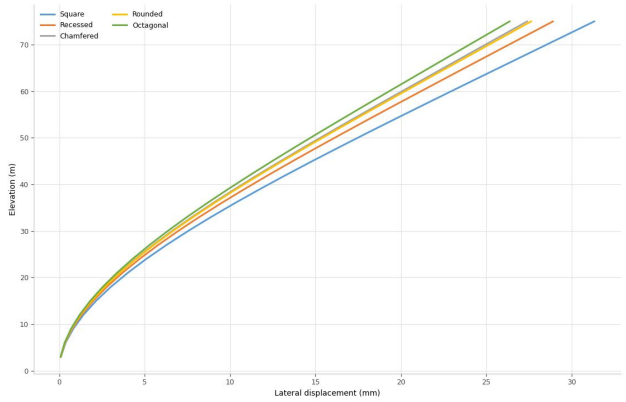


Fig. 7 Storey-Wise Lateral Displacement Profiles at 47 m/s

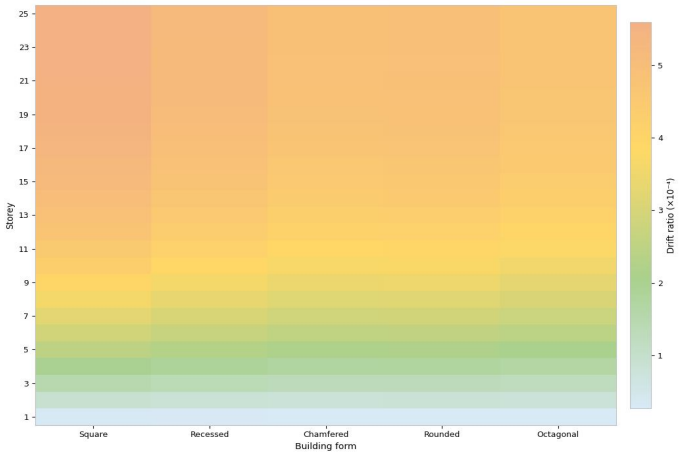


Fig. 8 Storey-Wise Drift Ratio Heatmap at 47 m/s

Displacement profiles indicate how the common height-varying floor-force distribution interacts with each form's overall bending rigidity. The elastic deflections are largest at the roof and are checked against global response values. For the 75 m reference form, the analytical roof deflection is 31.327 mm. Since the cantilever represents the structure by one equivalent EI, the profiles do not identify individual beam, wall or column deflection demands.

Inter-storey drift profiles describe local increments in the calculated deflection shape. Their smooth growth is mechanically consistent with the selected beam model; it is not a substitute for an ETABS drift assessment that includes the actual 25-storey floor and lateral-force-resisting system.

D. Storey Shear, Overturning Response and Aerodynamic Efficiency

Storey shear is the cumulative equivalent lateral force acting on and above each floor. Consequently, it is largest at the lowest storey and decreases towards the roof. Under W4, the base shears are 4,371.46 kN for the square, 3,961.22 kN for the recessed, 3,715.74 kN for the chamfered, 3,759.46 kN for the rounded and 3,513.98 kN for the octagonal form. Each shear curve is obtained from the same 25-floor wind-force integration, differing only through the adopted form coefficient.

The comparison of M3 and M4 illustrates the sensitivity of lateral action to the adopted geometry factor. The chamfered model develops 3,715.74 kN of base shear, compared with 3,759.46 kN for the rounded model, while the recessed alternative develops 3,961.22 kN. The octagonal model has the lowest global shear, 3,513.98 kN. Corresponding base overturning moments follow the same ranking: 151,222.71, 153,001.80, 161,212.99 and 143,011.52 kN·m, respectively. These moment values sum the individual floor forces multiplied by their centroid heights.

Overturning moment reflects both the magnitude and the height of the equivalent lateral wind forces. Under W4, the square reference produces 177,909.07 kN·m at the base, compared with 143,011.52 kN·m for the octagonal model, representing a 19.62% reduction. The recessed, chamfered and rounded alternatives yield 161,212.99, 151,222.71 and 153,001.80 kN·m, respectively. Each value is calculated by summing its 25 strip forces multiplied by the corresponding load-centroid elevations above the foundation. These external actions must later be evaluated against structural resistance, stabilizing gravity effects and governing design combinations.

The consistent reduction in base shear and overturning moment is caused by the assumed decrease in equivalent force coefficient while the vertical distribution of pressure remains fixed. The smaller displacement reductions reflect the concurrent changes in effective stiffness. This distinction prevents incorrectly attributing the results entirely to changes in airflow resolved by a numerical fluid simulation. The calculated effects remain appropriate as a controlled screening comparison, subject to aerodynamic and structural validation.

The expected flow behavior of each corner treatment allows for the following interpretation. A recess creates a local cavity that changes corner flow and moves the separation point. A chamfer, which replaces a sharp edge with a bevel, weakens suction concentrations and changes the direction of the separated flow. The shape of the chamfer plays a role in flow behavior and separation. A rounded edge changes the flow in a gradual manner and can prevent flow separation. The extent of flow separation is dependent on the radius of the curvature and the direction of the rounded edge. The optimum corner treatment is the octagonal shape, which breaks the dominance of the squared edge and reduces corner separation. Lu et al. (2024) studied the effects of using both the additive and the subtractive methods to adjust cross-sections of aerodynamic shapes and found that each shape changes the flow separation and the resulting wake. From a flow separation perspective, each of the treatments ranked in this study agrees with the general conclusion of Lu et al. (2024).

The present calculation does not resolve local pressure distributions, fluctuating wake forces or vortex-shedding frequencies. It is therefore not possible to deduce the direction-dependent dynamic wind response from global shear and moment values alone. Published studies show that corner or cross-sectional modifications can change aerodynamic loading mechanisms (Al-Masoodi et al., 2023; Lu et al., 2024), but the equivalent coefficients used here have not been independently calibrated against the detailed pressure field for this specific 25-storey geometry. Consequently, the results support comparative screening and indicate the need for direction-sensitive aerodynamic validation.

Reduced equivalent wind forces can lower the wind-related design actions that a lateral system must resist. However, an 19.62% calculated saving in the global shear or overturning moment does not establish the same proportional saving in concrete, reinforcement or foundation dimensions. Structural component sizes must also satisfy gravity, seismic, stability, drift and detailing requirements. The present results identify possible demand reductions for further design development; they do not quantify material savings or prove that supplemental damping and stiffness measures can be omitted.

The uppermost storey resists only the wind force assigned to its own floor strip, whereas the lowest storey carries the sum of the 25 equivalent wind forces. For the square form at w4 this summation gives 4,371.46 kn. The relative ordering of the five shear curves remains unchanged over height because each form uses the same pressure profile scaled by a constant force coefficient.

The overturning moment is calculated as the sum of individual floor forces multiplied by the heights of their loading centroids above the base. Under w4, the square plan gives 177,909.07 kn·m and the octagonal form gives 143,011.52 kn·m. these are external equivalent wind moments, not the factored stability capacity or foundation resistance of the building. Their interpretation must be supplemented by the appropriate design load combinations and foundation checks.

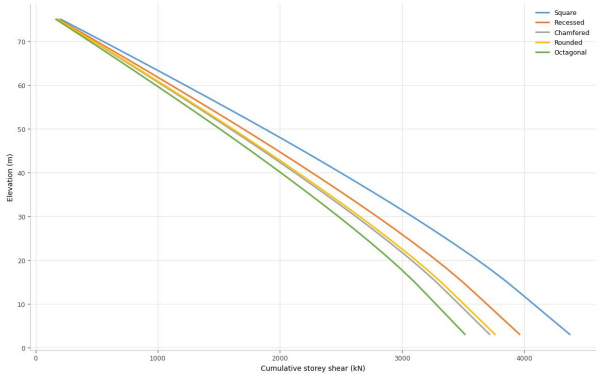


Fig. 9 Storey Shear Profiles and Square–Octagonal Difference at 47 m/s

E. Multi-Criteria Ranking and Selection of the Optimized Form

When evaluating candidate aerodynamic forms, multiple performance metrics should be considered. Base shear determines the magnitude and direction of the lateral force resisted by a structure. An overturning moment represents the effect of a lateral force on structure, and often occurs at a point of flexibility. Global flexibility is often defined by the highest point of a structure. Drift ratio determines the serviceability of a structure and determines the level of lateral movement of a structure.

A configuration that minimizes base shear does not necessarily minimize all other response measures. For this comparison, the five alternatives are ranked using base shear, overturning moment, roof displacement and maximum inter-storey drift ratio, all normalized to the square reference under the same 47 m/s wind case. The H/Δ ratio, calculated with H = 75,000 mm, offers a secondary description of the roof-displacement response. All rankings refer to the stated equivalent-static assumptions and are not final design acceptances.

In the W4 comparison the recessed treatment provides a 9.38% global-force reduction and a 7.72% displacement and drift reduction relative to the square reference. It is therefore a beneficial alternative in the controlled calculation but ranks fourth among the five forms when lowest demand is preferred. The rounded alternative performs better than recessing but remains marginally behind the chamfered form.

The chamfered configuration ranks second in the comparison. Its base shear and overturning moment decrease by 15.00% relative to the square form, and its roof displacement and maximum drift ratio decrease by 12.55%. The rounded configuration ranks third, with respective force and deformation savings of 14.00% and 11.79%. These rankings are conditional on the prescribed aerodynamic force coefficients and assumed effective stiffness values.

The octagonal model ranks first for all six wind cases in the present calculation. At W4 it reduces base shear by 19.62% and roof displacement and peak drift by 15.83% relative to M1, with a corresponding 19.62% reduction in overturning moment. The adopted coefficients generate the same relative savings at the other five wind intensities. Thus the result demonstrates stable performance under the selected equivalent-static assumptions rather than establishing an aerodynamic optimum independent of wind direction or pressure distributions.

The separation between the modified forms is relevant to engineering selection. At W4, the octagonal model's base shear is 201.76 kN lower than that of the chamfered option, while its roof displacement is 1.026 mm lower. Such differences may be significant during screening but cannot independently establish constructability, robustness or overall life-cycle suitability. The alternative should be selected only after comparing the actual structural framing changes and direction-sensitive wind load effects.

The six-wind comparison gives the same response ranking at every speed from 33 to 55 m/s. This reflects the common terrain profile, identical floor geometry and constant adopted form coefficients, not a direct study of variation in turbulent flow or vortex shedding. Independent testing of oblique winds and across-wind behavior could alter the ranking; the present result should be carried forward as a hypothesis for detailed wind and structural analysis.

Constructability and architectural function must be considered alongside the calculated wind response. A 12% octagonal treatment can influence perimeter geometry, floor planning and structural detailing more strongly than a 7.5% chamfer. Although the octagonal form ranks first for the assumed coefficients, the chamfered alternative may offer a practical trade-off if the architectural or construction effects of larger corner alterations are significant. Neither option can be selected for final design without geometry-specific wind assessment and detailed structural verification.

TABLE VII
AERODYNAMIC PERFORMANCE RANKING AT 47 M/S

Building form	Base shear red. (%)	Top disp. red. (%)	Drift red. (%)	H/Top disp.
Square (sharp corners)	0.00	0.00	0.00	2,394
Recessed corners	9.38	7.72	7.72	2,595
Chamfered corners	15.00	12.55	12.55	2,738
Rounded corners	14.00	11.79	11.79	2,714
Optimized octagonal corners	19.62	15.83	15.83	2,844

©IJRASET: All Rights are Reserved | SJ Impact Factor 7.538 | ISRA Journal Impact Factor 7.894 |

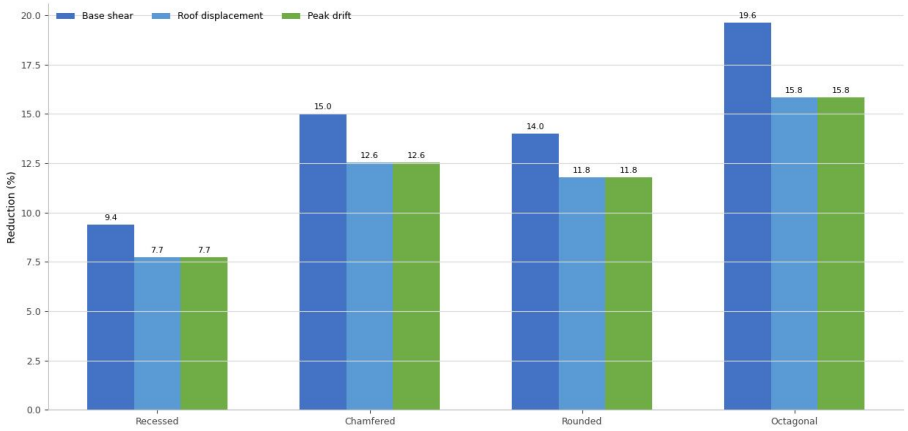


Fig. 10 Aerodynamic Response Reductions at 47 m/s

The form-selection process considers several response measures instead of relying solely on the smallest base shear. Under the adopted 25-storey calculation, the octagonal plan offers the lowest global force, overturning moment, roof displacement and peak drift, followed by the chamfered, rounded and recessed corner treatments. The H/Δ index reinforces this displacement ranking. These conclusions describe relative response within the defined analytical model and do not predetermine the most economical or constructible final solution.

Prioritizing a few solutions based on several design requirements gives more flexibility in making design choices. Solutions that excel in different requirements may give rise to other design choices including the choice of constructability. In cases where solutions exhibit favorable behaviors in many design requirements, these solutions should be established for further analysis and verification to assess whether aerodynamic design requirements are also met. From the rankings established, other design decisions may also need to be made. Of the solutions studied, it appears that the M5 solution was the best. It ranked the highest among other solutions based on the checks established. Because of this, verification of the solution to meet aerodynamic design requirements may be justified.

F. Engineering Interpretation, Literature Comparison and Limitations

The octagonal alternative provides the largest reduction among the five forms, but its calculated 19.62% decrease in base shear and 15.83% decrease in roof displacement and drift should not be equated with the larger reductions reported for different building models by Al-Masoodi et al. (2023). Published results depend on geometric details, flow conditions and analysis assumptions. The value of the current comparison is that it evaluates the same 75 m, 25-storey system with a consistent equivalent loading procedure.

The performance of rounded and chamfered corners in this work also agrees with the existing body of knowledge. The use of corner treatments to reduce mean wind effects and wind gusts has been documented. The amplitude of the benefits has been varying. It has been shown that the aerodynamic performance of chamfered corners can be improved by varying the ratio of the modification. Given the flow conditions and geometry of the building, it can be expected that rounded corners will perform better than chamfered corners. Other design variables, such as the radius of corner rounding, building aspect ratio, and flow conditions, can impact corner treatments and their order.

ETABS can evaluate spatial deformation, modal behavior, member actions, P-Delta effects and structural combinations when a complete model is available. In this study, the tabulated numerical values are obtained from an equivalent elastic cantilever rather than a documented three-dimensional ETABS analysis. Accordingly, the computed quantities should be regarded as preliminary reference values for subsequent ETABS calibration. Geometry-specific wind pressures, material and member properties, diaphragm behavior, dynamic response and overall serviceability must be confirmed independently.

The analysis assumes a single wind direction, a common 30 m windward width, prescribed form coefficients, uniformly distributed floor weight and a fixed-base equivalent stiffness. It excludes torsional effects, across-wind resonance, directional aerodynamic interactions, detailed cladding pressures, member design and soil–structure interaction. The results therefore support comparative screening of five 25-storey geometries but cannot establish that any form meets all requirements of IS 875 (Part 3):2015 or the structural design codes.

The equivalent stiffness values are assumed rather than derived from independently detailed and verified structural member sections. Therefore, the calculated response differences reflect the joint effect of the specified aerodynamic coefficients and EI multipliers. Future work should resolve corner coordinates, determine local wind pressure distributions, construct consistent ETABS models, check load combinations and modal participation, and investigate across-wind and torsional responses. Only then can any asserted aerodynamic benefits be accepted for final design.

Within the limits of the 75 m, 25-storey comparison, M5 is the most favorable form for the selected wind direction and six basic wind speeds. Its consistent advantage makes it a reasonable candidate for further evaluation, alongside the chamfered configuration. This result is not an engineering approval of the final building design: complete wind-action validation and three-dimensional structural verification are required before selecting member sizes or declaring compliance.

There are consequences relating to the timing of engineering decisions. If the aerodynamic form of the building is evaluated before the lateral system is substantially strengthened, the design team can discern if the change in geometry is actually reducing the demands of the wind. If improved response of the building is primarily the result of lateral system stiffness, then the conclusions drawn by the design team are of little value. Furthermore, with the lateral system stiffness balancing demands of the wind, the architectural and structural design decisions can be made in parallel. The decisions of the architectural design can inform the decisions of the structural design and vice versa. If the lateral system of the building is designed based on the principles of CFD or wind tunnel tests, the final design of the building members can be based on the results of the CFD or wind tunnel tests. In all other cases, the comparison of CFD or wind tunnel tests can be done using updated pressure conditions.

The changes in the geometry of the building, as described above, are consistent with the behavior described in the literature review. Removal of corner constraints of a building is expected to relieve load. The other geometrical changes described above, especially the use of chamfered corners, are expected to reduce the overall demands of the wind on the building. The use of the rounded corners of a building also is expected to relieve the demands of the wind.

The nearby ranking of the chamfered and rounded alternatives illustrates the need for caution. At W4 their base shears differ by only 43.71 kN, and their roof displacements differ by about 0.237 mm. Given the simplifying assumptions of the equivalent cantilever and the adopted force coefficients, this difference is insufficient to claim an inherently superior real-world flow behavior without further aerodynamic evidence. The ranking should guide, rather than replace, subsequent geometry-resolved testing.

G. Consolidated Global Results and Modelling Interpretation

The W4 comparative results show that the adopted corner treatments progressively reduce equivalent wind actions relative to the square reference, although the chamfered case is slightly more favorable than rounding. Base shear decreases from 4,371.46 kN for M1 to 3,513.98 kN for M5; overturning moment decreases from 177,909.07 to 143,011.52 kN·m. Roof displacement decreases from 31.327 to 26.368 mm, and maximum inter-storey drift ratio decreases from 0.000560 to 0.000471. These are equivalent-cantilever results for a 25-storey, 75 m building, not verified ETABS model exports.

The approximate modal periods range from 1.736 s for M1 to 1.777 s for M5, reflecting the different assumed equivalent EI values. Force reductions are directly linked to the adopted coefficients; the resulting displacement and drift changes also reflect model stiffness. Consequently, the consolidated comparison establishes transparent relative behavior under the stated assumptions but leaves complete structural and aerodynamic validation to a later ETABS and wind-assessment stage.

TABLE VIII
AERODYNAMIC PERFORMANCE RANKING AT 47 M/S

Model	Base shear (kN)	OTM (kN·m)	Roof displacement (mm)	Max drift ratio	T1 (s)
M1 - Square	4,371.46	177,909.07	31.327	0.000560	1.736
M2 - Recessed	3,961.22	161,212.99	28.907	0.000517	1.752
M3 - Chamfered	3,715.74	151,222.71	27.395	0.000490	1.761
M4 - Rounded	3,759.46	153,001.80	27.632	0.000494	1.759
M5 - Optimized octagonal	3,513.98	143,011.52	26.368	0.000471	1.777

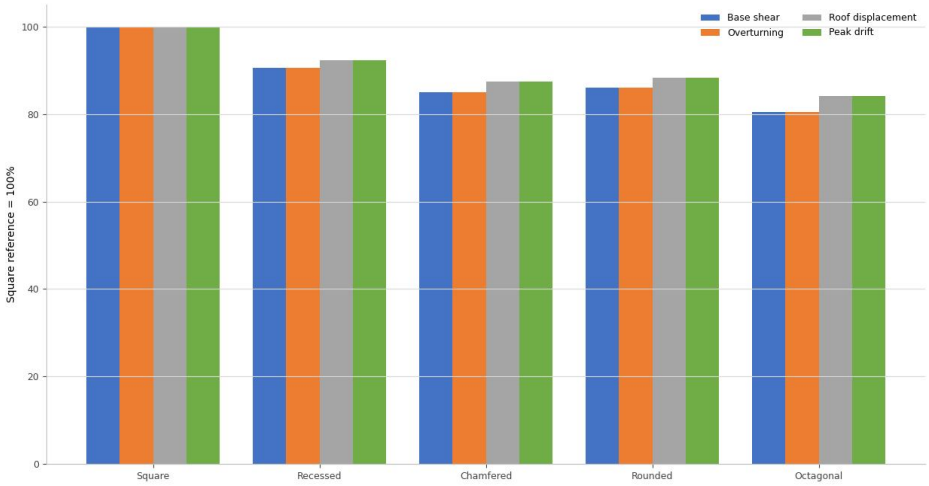


Fig. 11 Normalized Global Responses at 47 m/s

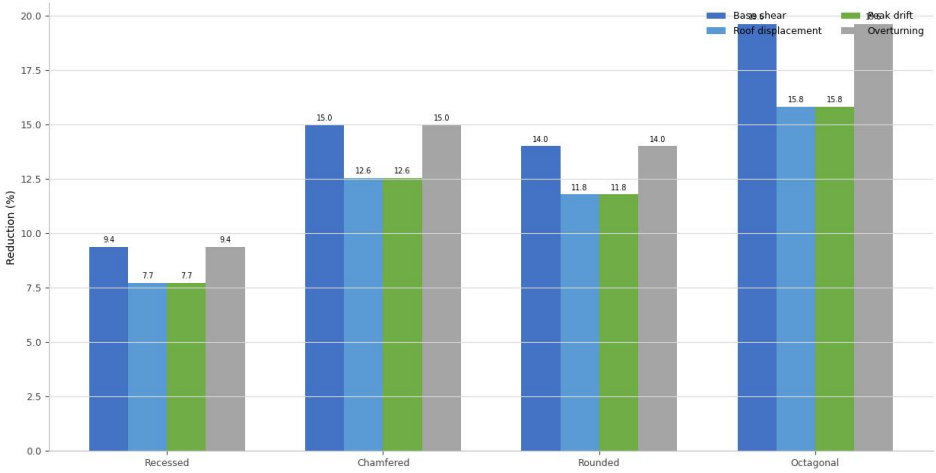


Fig 12 Global Response Reductions Relative to Square Reference

REFERENCES

[1] A. Sharma, H. Mittal, A. Gairola (2018). "Mitigation of wind load on tall buildings through aerodynamic modifications: Review." Journal of Building Engineering, 18, 180-194. https://doi.org/10.1016/j.jobe.2018.03.005

[2] A.H.H. Al-Masoodi, Y.M. Abbas, F. Alkhatib, M.I. Khan, N. Shafiq, M. ElGawady (2023). "Aerodynamic optimization for corner modification of octagonal-shape tall buildings using computational approach." Journal of Building Engineering, 76, 107017. https://doi.org/10.1016/j.jobe.2023.107017

[3] S. Li, Y. Deng, Z. Zhong, Z. Chen (2023). "Effects of corner modifications on wind-induced responses of super high-rise buildings by wind tunnel tests based on a novel low-damping elastic test model." Journal of Building Engineering, 67, 105881. https://doi.org/10.1016/j.jobe.2023.105881

[4] W.-T. Lu, B.M. Phillips, Z. Jiang (2024). "Aerodynamic responses of tall buildings with cross-section modification through additive- and subtractive-based strategies." Journal of Wind Engineering and Industrial Aerodynamics, 250, 105762. https://doi.org/10.1016/j.jweia.2024.105762

[5] A. Elshaer, G.T. Bitsuamlak, A. El Damatty (2017). "Enhancing wind performance of tall buildings using corner aerodynamic optimization." Engineering Structures, 136, 133-148. https://doi.org/10.1016/j.engstruct.2017.01.019

[6] Y. Li, X. Tian, K.F. Tee, Q.-S. Li, Y.-G. Li (2018). "Aerodynamic treatments for reduction of wind loads on high-rise buildings." Journal of Wind Engineering and Industrial Aerodynamics, 172, 107-115. https://doi.org/10.1016/j.jweia.2017.11.006

[7] Y. Li, Y.-G. Li, Q.-S. Li, K.-F. Tee (2019). "Investigation of wind effect reduction on square high-rise buildings by corner modification." Advances in Structural Engineering, 22(6). https://doi.org/10.1177/1369433218816111

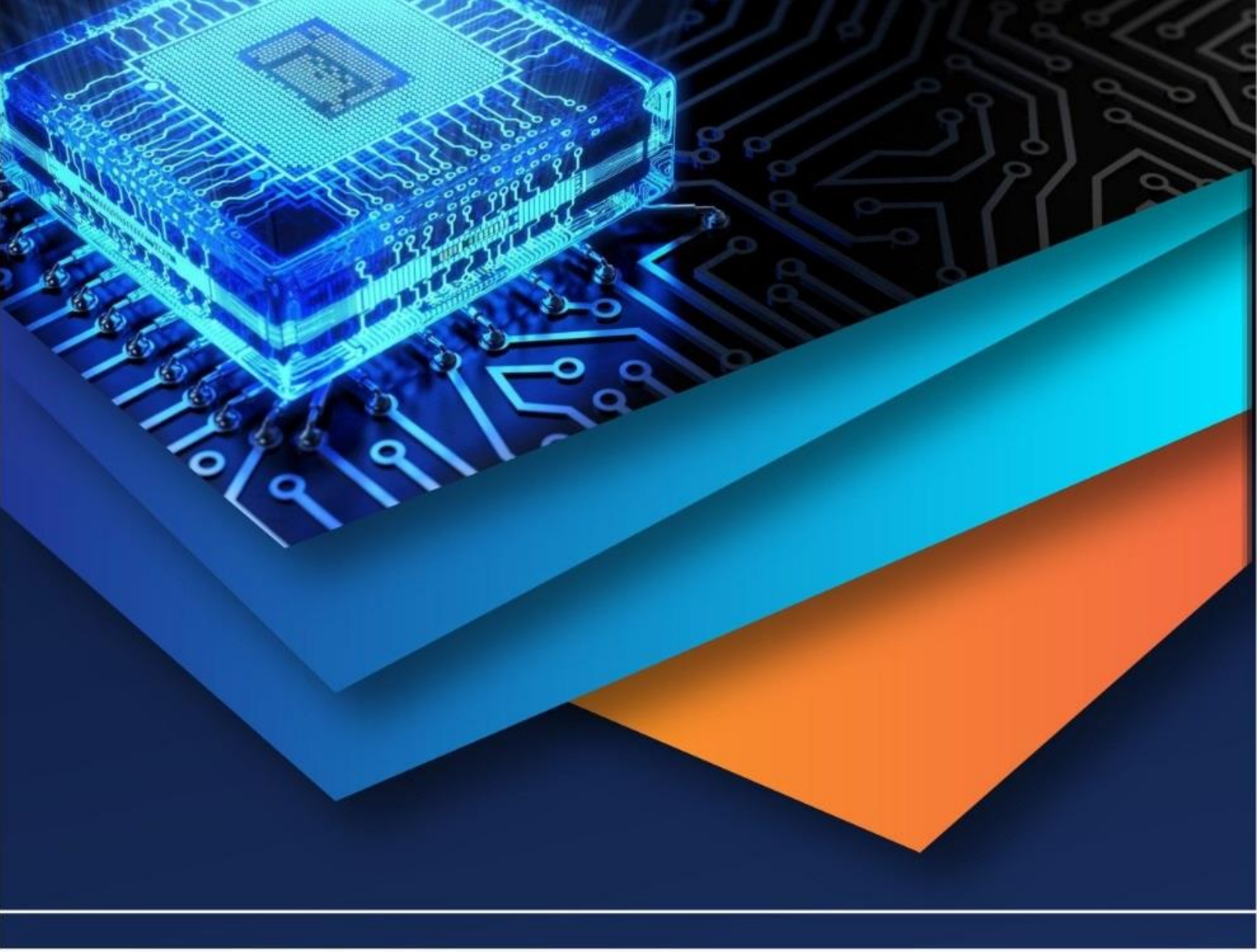
[8] Y. Li, C. Li, Q.-S. Li, Q. Song, X. Huang, Y.-G. Li (2020). "Aerodynamic performance of CAARC standard tall building model by various corner chamfers." Journal of Wind Engineering and Industrial Aerodynamics, 202, 104197. https://doi.org/10.1016/j.jweia.2020.104197

[9] G.W. Alminhana, A.L. Braun, A.M. Loredo-Souza (2018). "A numerical-experimental investigation on the aerodynamic performance of CAARC building models with geometric modifications." Journal of Wind Engineering and Industrial Aerodynamics, 180, 34-48. https://doi.org/10.1016/j.jweia.2018.07.001

[10] M. Mooneghi, B. Kargarmoakhar (2016). "Aerodynamic Mitigation and Shape Optimization of Buildings: Review." Journal of Building Engineering, 6, 225-235. https://doi.org/10.1016/j.jobe.2016.01.009

[11] M. Jafari, A. Alipour (2021). "Methodologies to mitigate wind-induced vibration of tall buildings: A state-of-the-art review." Journal of Building Engineering, 33, 101582. https://doi.org/10.1016/j.jobe.2020.101582
[12] M. Jafari, A. Alipour (2021). "Aerodynamic shape optimization of rectangular and elliptical double-skin façades to mitigate wind-induced effects on tall buildings." Journal of Wind Engineering and Industrial Aerodynamics, 213, 104586. https://doi.org/10.1016/j.jweia.2021.104586
[13] M.S. Thordal, J.C. Bennetsen, H.H. Koss (2019). "Review for practical application of CFD for the determination of wind load on high-rise buildings." Journal of Wind Engineering and Industrial Aerodynamics, 186, 155-168. https://doi.org/10.1016/j.jweia.2018.12.019
[14] P. Sanyal, S.K. Dalui (2020). "Effect of corner modifications on Y plan shaped tall building under wind load." Wind and Structures, 30(3), 245-260. https://doi.org/10.12989/was.2020.30.3.245
[15] S. Mandal, S.K. Dalui, S. Bhattacharjya (2021). "Wind induced response of corner modified U plan shaped tall building." Wind and Structures, 32(6), 521-537. https://doi.org/10.12989/was.2021.32.6.521
[16] S. Bhattacharya, S.K. Dalui (2022). "Effect of Aerodynamic Modification on V plan Shaped Tall Building Under Wind Excitation." ASPS Conference Proceedings, 1(5). https://doi.org/10.38208/acp.v1.679
[17] S. Mandal, S.K. Dalui, S. Bhattacharjya (2022). "Wind-Induced effect on different corner positions of corner-modified irregular plan-shaped tall building." Lecture Notes in Mechanical Engineering, 311-323. https://doi.org/10.1007/978-981-16-6738-1_26
[18] K.T. Tse, G. Hu, C. Song, H.S. Park, Y.C. Kim (2021). "Effects of corner modifications on wind loads and local pressures on walls of tall buildings." Building Simulation, 14(4), 1109-1126. https://doi.org/10.1007/s12273-020-0705-3
[19] F. Alkhatib, N. Kasim, W.I. Goh, N. Shafiq, M. Amran, E.V. Kotov, M.A. Albaom (2022). "Computational Aerodynamic Optimization of Wind-Sensitive Irregular Tall Buildings." Buildings, 12(7), 939. https://doi.org/10.3390/buildings12070939
[20] X. Xu, Q. Yang, A. Yoshida, Y. Tamura (2017). "Characteristics of pedestrian-level wind around super-tall buildings with various configurations." Journal of Wind Engineering and Industrial Aerodynamics, 166, 61-73. https://doi.org/10.1016/j.jweia.2017.03.013
[21] Y. Tamura, X. Xu, H. Tanaka, Y.C. Kim, A. Yoshida, Q. Yang (2017). "Aerodynamic and Pedestrian-Level Wind Characteristics of Super-Tall Buildings with Various Configurations." Procedia Engineering, 199, 28-37. https://doi.org/10.1016/j.proeng.2017.09.146
[22] T. Deng, J. Fu, Q. Zheng, J. Wu, et al. (2019). "Performance-Based Wind-Resistant Optimization Design for Tall Building Structures." Journal of Structural Engineering, 145(10), 04019103. https://doi.org/10.1061/(ASCE)ST.1943-541X.0002383
[23] M.A. Bezabeh, G.T. Bitsuamlak, S. Tesfamariam (2020). "Performance-based wind design of tall buildings: concepts, frameworks, and opportunities." Wind and Structures, 31(2), 103-142. https://doi.org/10.12989/was.2020.31.2.103
[24] W. Cui, L. Caracoglia (2020). "Performance-based wind engineering of tall buildings examining life-cycle downtime and multisource wind damage." Journal of Structural Engineering, 146(1), 04019179. https://doi.org/10.1061/(ASCE)ST.1943-541X.0002479
[25] J. Wu (2019). "Dynamic performance evaluation of Shanghai Tower under winds based on full-scale data." The Structural Design of Tall and Special Buildings, 28, e1611. https://doi.org/10.1002/tal.1611
[26] Y.-H. Juan, A. Rezaeiha, H. Montazeri, B. Blocken, A.-S. Yang (2024). "Improvement of wind energy potential through building corner modifications in compact urban areas." Journal of Wind Engineering and Industrial Aerodynamics, 248, 105710. https://doi.org/10.1016/j.jweia.2024.105710
[27] A. Baghaei Daemei, E.M. Eghbali, M. Khotbehsara (2019). "Study on wind aerodynamic and flow characteristics of triangular-shaped tall buildings and CFD simulation in order to assess drag coefficient." Ain Shams Engineering Journal, 10(3), 541-548. https://doi.org/10.1016/j.asej.2018.08.008
[28] E. Bernardini, S.M.J. Spence, D. Wei, A. Kareem (2015). "Aerodynamic shape optimization of civil structures: A CFD-enabled Kriging-based approach." Journal of Wind Engineering and Industrial Aerodynamics, 144, 154-164. https://doi.org/10.1016/j.jweia.2015.03.011
[29] S. Tanios (2016). "Structural Design and Analysis of High-Rise Buildings Subject to Seismic and Wind Loads: A Case Study." Master of Engineering Thesis, Lebanese University, Faculty of Engineering - Branch II. https://doi.org/10.13140/RG.2.2.33414.70725/1
[30] Bureau of Indian Standards (2015). IS 875 (Part 3):2015, Design Loads (Other than Earthquake) for Buildings and Structures - Code of Practice, Part 3: Wind Loads (Third Revision). New Delhi: Bureau of Indian Standards.

©IJRASET: All Rights are Reserved | SJ Impact Factor 7.538 | ISRA Journal Impact Factor 7.894 |



10.22214/IJRASET

45.98

IMPACT FACTOR: 7.129

IMPACT FACTOR: 7.429

INTERNATIONAL JOURNAL FOR RESEARCH

IN APPLIED SCIENCE & ENGINEERING TECHNOLOGY

Call : 08813907089 (24*7 Support on Whatsapp)